Polymer Journal, Vol. 16, No. 12, pp 857—866 (1984)

# Study on the Solubility of Cellulose in Aqueous Alkali Solution by Deuteration IR and $^{13}C$ NMR

Kenji KAMIDE, Kunihiko OKAJIMA, Toshihiko MATSUI, and Keisuke KOWSAKA

*Textile Research Laboratory, Asahi Chemical Industry Co., Ltd., Takatsuki, Osaka 569, Japan*

(Received March 14, 1984)

ABSTRACT: A correlation of the solubility of cellulose in aqueous alkali solution was established with its so-called "amorphous" content. To achieve this end, cellulose was regenerated under different preparative conditions from its cuprammonium solution and cotton linter was acid-hydrolyzed into a fibrous form and the pulp was physically milled to powder. Cellulose having a relatively large molecular weight was found to completely dissolve in aqueous NaOH solution at 4°C. The solubility of cellulose in a 10 wt% aqueous NaOH at 4°C, $S_a$ could generally be correlated to the relative amount of the high magnetic field envelope of the $C_4$ carbon NMR peak, $\chi_h$ (NMR). $\chi_h$ (NMR) was assigned to the region where intramolecular hydrogen bonds are at least partly broken. The intramolecular hydrogen bond was found to have an important influence on the solubility behavior of cellulose.

KEY WORDS Cellulose / Regenerated Cellulose / Cuprammonium Solution / NaOH Solution / Solubility / X-Ray Diffraction Method / Deuteration IR Method / CP-MASS $^{13}C$ NMR Spectroscopy /

Since Mercel discovered the process of the so-called mercerization of cellulose, a process imparting to cotton fabrics by treating cellulose with aqueous alkali solution under tension, the swelling phenomena of cellulose with aqueous alkali solution has long been studied in some detail, by many investigators. For example, for natural cellulose, about 8—10 wt% aqueous sodium hydroxide (NaOH) at low temperature was found experimentally to be the most powerful swelling agent[1,2] in which only a small part (probably, a low molecular weight compound) of cellulose can be dissolved.[3-6] Staudinger *et al.*[5] described, without giving the details, that cotton and mercerized cotton can dissolve in a 10% (w/v) NaOH solution when their viscosity average degrees of polymerization ($P_v$) are below 400, and regenerated cotton with $P_v$ of less than 1200 can also dissolve in 10% (w/v) NaOH. The solubility behavior of the regenerated cellulose observed by Staudinger *et al.* was unfortunately not reproducible. Viscose and cuprammonium rayons never dissolve completely in 10% (w/v) aqueous NaOH. The word "löslichkeit in 10-iger NaOH," which Staudinger used in his study should be understood to mean partial dissolution. The experimental fact that cellulose contains the alkali soluble part was used to evaluate the lateral order distribution of cellulose fibers without seriously considering the molecular weight fractionation effect by the alkali. In this case, it has been accepted without direct evidence that only the difference in the aggregate state of cellulose molecular chains influences predominantly the solubility of cellulose towards alkali. From a theoretical view point, the cellulose molecular chains influences predominantly the solubility of cellulose towards in water if there are no intra- and intermolecular hydrogen bonds. Discussion of the

solubility of cellulose from view points of both the aggregate state of the molecular chain and hydrogen bonding seems useful, but needs further detailed experimental evidence. Recent advance in high resolution NMR technique, especially in the cross-polarization magic angle sample spinning (CP-MASS) $^{13}C$ NMR technique for solid cellulose[7-15] will facilitate the solution of the problem of the solubility of cellulose in aqueous NaOH.

In this paper, we show that regenerated cellulose prepared under special conditions is completely soluble in a 10 wt% aqueous NaOH at 4°C and discuss the solubility of cellulose in terms of intramolecular hydrogen bonding using CP-MASS $^{13}C$ NMR and deuteration IR.

## EXPERIMENTAL

### *Cellulose Samples*

Four regenerated cellulose sample films were prepared as follows. A cellulose solution (cellulose concentration: 8 wt%) was made by dissolving purified cotton (viscosity-average molecular weight $M_v = 19.4 \times 10^4$) in cuprammonium solution. The resulting solution composition (molar ratio) was cellulose/$NH_3$/Cu/$H_2O$ = 1.0/6.4/1.0/75.6. The solution was cast on a glass plate and then immediately dipped into a 5 wt% aqueous sulfuric acid ($H_2SO_4$) bath at 28°C, washed and dried in air. During this procedure, coagulation and regeneration seem to occur almost simultaneously. The film thus prepared was coded as BRC-1. Sample BRC-2 and BRC-4 films were obtained by casting the cellulose solution on glass plates and partially evaporating ammonia from the cast solutions in air at 25°C for 3 min and 120 min, respectively, dipping them in a 2 wt% aqueous $H_2SO_4$ at 25°C for 20 min, followed by washing with water and drying in air. We obtained the BRC-3 film by dipping BRC-2 film into water at 25°C for 24 h, followed by drying in air. A regenerated cellulose solid mass sample coded as BRC-5 was obtained as follows. The cellulose solution was poured into acetone with strong agitation and the coagulated precipitate was separated by filtration. The precipitate was regenerated with a 2 wt% aqueous $H_2SO_4$ at 25°C for 20 min, followed by washing with water and drying in air. BRC-1—BRC-4 were subjected to X-ray diffraction, deuteration IR spectroscopy, CP-MASS $^{13}C$ NMR spectroscopy and a solubility test. BRC-5 was subjected only to the X-ray diffraction and the solubility test.

Three acid-hydrolyzed cotton samples (CL-1, CL-2, CL-3) treated with 6 wt% aqueous $H_2SO_4$ at 60°C for 0 to 120 min) and the powdered pulp (PC-1) obtained by ball milling were also subjected to X-ray diffraction and the solubility test. The CP-MASS $^{13}C$ NMR spectrum was recorded for PC-1.

For polarized IR spectroscopy, the oriented film samples for BRC-1 and BRC-4 were prepared as follows. A wet BRC film containing 300% water was stretched in one direction by 200% and fixed in that state and finally dried in air. BRC-4 oriented film was obtained by same procedure above except it was stretched 300%.

### *Viscosity-Average Molecular Weight*

$M_v$ of the samples and the starting cellulose materials were calculated from following equation[16]

$$[\eta] = 3.85 \times 10^{-2} M_w^{0.76} \text{ in cadoxen at } 25°C \quad (1)$$

Here, $M_w$ is the weight-average molecular weight.

### *X-Ray Diffraction*

X-Ray diffraction patterns of the samples were recorded by the transmission method with a RU-200PL type X-ray diffractometer (Rigaku Denki Co., Japan). The crystallinity $\chi_c(X)$ of the samples was a calculated by the equation proposed by Segal.[17]

$$\chi_c(X) = \frac{I_{002} - I_{am}}{I_{002}} \quad (2)$$

where $I_{002}$ is the diffraction intensity for the peak ($2\theta=21.7°$) of the plane (002), and $I_{am}$, the intensity at $2\theta \doteq 16°$ for cellulose II. For cellulose I, $I_{002}$ is the intensity for the peak at $2\theta=22.6°$ and $I_{am}$, that at $2\theta=19°$. We defined the degree of amorphous content of the samples $\chi_{am}(X)$ by eq 3

$$\chi_{am}(X)=1-\chi_c(X) \tag{3}$$

*Deuteration IR*

IR spectra of the sample and partially deuterated sample films were recorded with an IR spectrometer model 430 special (Shimadzu Co., Japan), using a deuteration cell designed and constructed at our laboratory for this purpose. Deuteration of the sample was carried out by passing $D_2O$ vapor into the cell for 180 min to attain deuteration equilibrium. During deuteration the sample holder was kept at $100\pm0.5°C$. The fraction of the accessible part $\chi_{ac}(IR)$ at equilibrium was calculated by the equations proposed by Mann *et al.*[18]

$$\log(I_0/I)_{OD}/\log(I_0/I)_{OH} = 1.11\times C_{OD}/C_{OH} \tag{4}$$

$$C_{OD}+C_{OH}=1 \tag{5}$$

Here $(I_0/I)_{OH}$ and $(I_0/I)_{OD}$ are the maximum optical density at the OH stretching region (3440—3370 $cm^{-1}$) and OD stretching region (2490—2520 $cm^{-1}$), respectively. $C_{OD}$ and $C_{OH}$ are the fractions of the accessible and inaccessible parts at equilibrium, respectively. Hence, $C_{OD}$ directly gives $\chi_{ac}(IR)$.

*NMR Spectroscopy*

CP-MASS $^{13}C$ NMR spectra of the cellulose samples were recorded with an FT NMR spectrometer FX-200 (50.1 MHz) (JEOL, Japan) under the following conditions: 90° pulse, pulse width; 4.5 $\mu$s, pulse repetition; 5 s, pulse interval (cross-polarization contact time); 1—2 $\mu$s, data point; 8 k.

For the BRC-4 solution in NaOH–$D_2O$ (10 : 90, w/w) (polymer concentration; 5 wt%), the $^{13}C$ NMR spectrum was obtained using same spectrometer and operating conditions above. The relative amount of the higher field peaks $\chi_h(NMR)$ of the $C_4$ carbon peaks was estimated from eq 7

$$\chi_h(NMR)=I_h/(I_l+I_h) \tag{7}$$

Here, $I_l$ and $I_h$ denote peak areas under the peaks centered at 87.9 and 84 ppm, respectively and the line shapes were approximated as the Lorenzian type.

*Solubility Test*

The cellulose film samples were scissored into small pieces, 5 mm × 5 mm, and vacuum-dried at 40°C for 18 h. Into 99—95 parts of 1—15 wt% aqueous NaOH precooled at 4°C, 1—5 parts of the cellulose were dispersed for 1 h at 4°C and quickly distributed using a home mixer intermittently in 1 min to minimize the rise in local temperature. The dispersed solution was then subjected to ultra-centrifuge at 20,000 rpm at 4°C for 45 min, followed by measuring the amount of cellulose ($m_G$) in the remaining gelatinous layer (lower liquid phase) by regeneration. This procedure was also applied to the BRC-5 and natural cellulose samples. The solubility of cellulose $S_a$ is defined by eq 8.

$$S_a=(m_0-m_G)/m_0 \tag{8}$$

where $m_0$ denotes the amount of cellulose originally used in this test.

## RESULTS

Figure 1 shows the X-ray diffraction patterns of the cellulose samples. As expected, all the regenerated cellulose samples had the crystalline form of cellulose II, showing typical diffraction peaks for the plane (002) at $2\theta=21.7°$ (Fig. 1a) and the acid-hydrolyzed cotton (CL series) and the powdered pulp (PC-1) (Fig. 1b) was comprised of the cellulose I type crystals with typical diffraction peaks for the

**Table I.** Molecular characteristics of cellulose samples

| Sample | Crystal form | $M_v \times 10^{-4}$ | $S_a$[a] / % | $\chi_{am}$(X) | $\chi_{ac}$(IR) | $\chi_h$(NMR) |
|---|---|---|---|---|---|---|
| BRC-1 | II | 8.1 | 52 | 0.46 | 0.59 | 0.56 |
| BRC-2 | II | 7.9 | 62 | 0.69 | 0.68 | 0.62 |
| BRC-3 | II | 7.9 | 81 | 0.88 | 0.64 | 0.79 |
| BRC-4 | II | 7.9 | 90 | 0.73 | 0.68 | 0.87 |
| BRC-5 | II | 7.9 | 100 | 0.94 | — | — |
| CL-1 | I | 19.4 | 9 | 0.21 | — | — |
| CL-2 | I | 8.3 | 31 | 0.25 | — | — |
| CL-3 | I | 5.8 | 30 | 0.26 | — | — |
| PC-1 | I | 1.9 | 58 | 0.92 | — | — |

[a] Measured at initial polymer concentration $C=5$ (wt%) for a 10 wt% aqueous NaOH at 4°C.

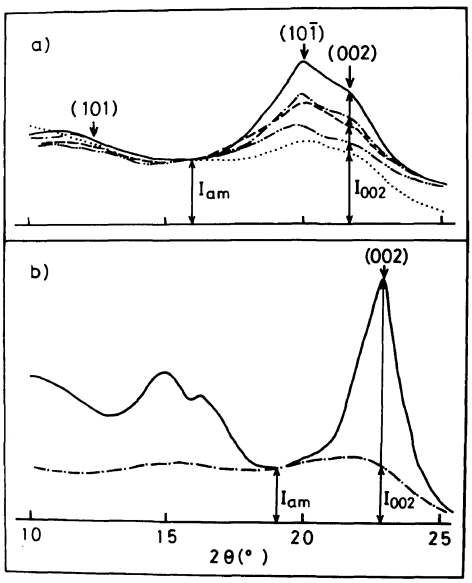


**Figure 1.** X-Ray diffraction patterns for regenerated (a) and natural (b) celluloses. (a) ——, BRC-1; — · —, BRC-2; — — —, BRC-3, – – –, BRC-4; ------, BRC-5; (b) ——, CL-1; — · —, PC-1.

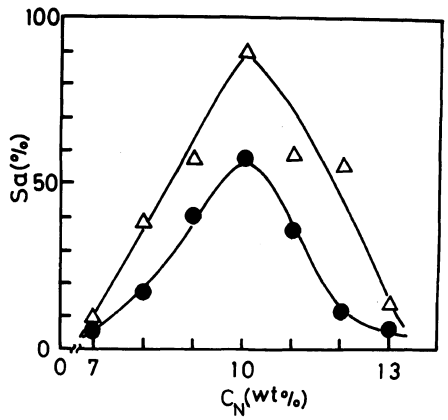


**Figure 2.** Relationship between solubility $S_a$ of cellulose at 4°C and NaOH concentration $C_N$ (wt%) in water as the solvent: △, BRC-4; ●, PC-1.

plane (002) at $2\theta=22.6°$. The 2nd and 5th columns of Table I show the results for the crystal forms and the so-called amorphous content $\chi_{am}$(X), respectively. $\chi_{am}$(X) for the BRC series samples ranges from 0.46 to 0.88 and that of the CL series is about the same ($0.23\pm0.03$). PC-1 was nearly amorphous ($\chi_{am}(X)=0.92$).

The $M_v$ data appear in the 3rd column of Table I. $M_v$ of the regenerated samples are nearly all about the same ($8.0\pm0.1\times10^4$). Those of the CL series range from 5.8—$19.4\times10^4$ and that of PC-1, as low as $1.9\times10^4$.

Figure 2 shows the effect of NaOH concentration $C_N$ (wt%) of the aqueous NaOH solution on $S_a$ at the initial polymer concentration $C_p=5$ wt% at 4°C of samples BRC-4 (unfilled mark) and PC-1 (filled mark). Obviously, the 10 wt% aqueous NaOH is the most potent solvent towards cellulose. The NaOH concentration dependence of $S_a$ seems independent of the crystalline form.

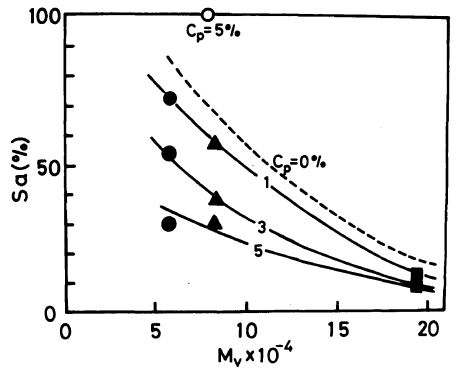


**Figure 3.** Dependence of solubility $S_a$ of natural cellulose in a 10 wt% aqueous NaOH at 4°C on viscosity-average molecular weight $M_v$: ■, CL-1; ▲, CL-2; ●, CL-3; ○, BRS-5. $C_p$ on the lines denotes the initial concentration (wt%) of cellulose in a 10 wt% aqueous NaOH and the broken line was drawn by extrapolating $C_p$ to 0, from Figure 4.

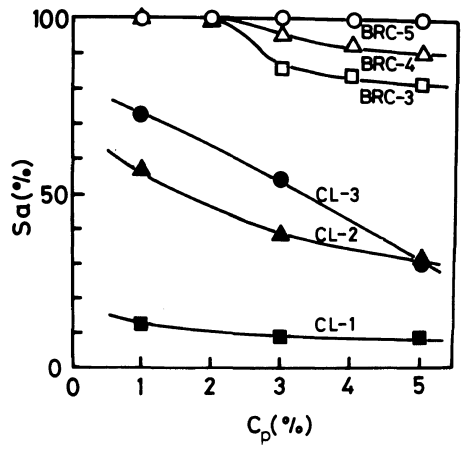


**Figure 4.** Initial concentration $C_p$ dependence of solubility $S_a$ of cellulose samples in a 10 wt% aqueous NaOH at 4°C: □, BRC-3; △, BRC-4; ○, BRC-5; ■, CL-1; ▲, CL-2; ●, CL-3.

Figure 3 shows the dependence of $S_a$ on $M_v$ for the CL series (cotton linter) having nearly the same $\chi_{am}(X)$ value for the 10 wt% aqueous NaOH at 4°C. Numbers on the lines denote the polymer concentration $C_p$ (wt%) initially charged in the alkali. $S_a$ drops below 15% irrespective of $C_p$ when $M_v$ of the polymer increases. $S_a$ increases with a decrease in $M_v$ and $C_p$: $S_a$ for cotton having $M_v = 5.8 \times 10^4$ was 72.5% at $C_p = 1$ wt%. In the figure, the broken line was drawn from a line of $S_a$ extrapolated to $C_p = 0$%. Thus, the solubility of natural cellulose in alkali strongly depends on both $M_v$ and $C_p$.

Figure 4 shows the dependence of $S_a$ on the $C_p$ of cellulose samples for a 10 wt% aqueous NaOH at 4°C. In the figure the unfilled marks denote BRC series samples and filled marks, the cotton (CL series). The dependence for BRC series is not so large as that of the CL series samples. BRC series samples prepared in this study had higher alkali solubility than cotton when compared at the same $M_w$ (about $8 \times 10^4$). In particular, sample BRC-5 was completely soluble when the $C_p$ below 5 wt%. In the 4th column of Table I, $S_a$ for a 10 wt% aqueous NaOH at $C_p = 5$ wt% at 4°C are shown. The regenerated cellulose, prepared by changing the vaporization time of ammonia from the cuprammonium cellulose solution and the precipitation method of cellulose reveals a large variety of $S_a$. That is, $S_a$ decreases from 100 to 52% in the following order: BRC-5 > BRC-4 > BRC-3 > BRC-2 > BRC-1. $S_a$ of the natural cellulose was at most 58% (for PC-1). The difference in $S_a$ for these regenerated samples might be correlated to the difference in the supermolecular structure of the samples.

Figure 5 exemplifies typical infrared spectra of the deuterated and non-deuterated samples BRC-1 and -4. $\chi_{ac}$(IR) evaluated using eq 4 and 5 from spectra is summarized in the 6th column of Table I. $\chi_{ac}$(IR) ranges from 0.59—0.68 and is essentially the same for any samples.

Figure 6 shows the CP-MASS $^{13}C$-NMR spectra for the samples. Assignment of the spectra was made with the aid of previous works by Earl *et al.*[8,9] and is given in Table II. Depending on the preparative method, $C_1$, $C_4$ and $C_6$ carbon peaks change systematically and in particular, variation in the $C_4$ carbon peak is remarkable. Therefore, we analyzed the $C_4$ carbon peak region using the method

**Table II.** NMR peak assignments (in ppm)

| Sample | Peak position[a] | | | |
|---|---|---|---|---|
| | $C_1$ | $C_4$ | $C_5$, $C_3$, $C_2$ | $C_6$ |
| BRC-1 | 107.3, 105.4, 97.5 | 87.9*, 83.8, 81.7 | 75.1 (broad) | 63.1, 61.0, 60.0 |
| BRC-2 | 107.3, 105.3, 104.3 | 88.8*, 87.9*, 85.3 | 75.2 (broad) | 63.0 |
| | | 84.3, 83.6, 82.8 | | |
| BRC-3 | 107.3, 105.3, 98.0 | 89.8*, 87.7*, 86.4 | 75.1 (broad) | 62.9, 60.5 |
| | 97.7 | 85.8, 85.0, 84.0 | | |
| | | 82.3, 81.7, 80.6 | | |
| BRC-4 | 107.3, 105.2, 100.5 | 87.8*, 85.3, 84.2 | 75.3 (broad) | 62.8, 61.8, 60.7 |
| | 97.3 | 82.6, 81.8 | | 60.0 |
| PC-1 | 105.4, 104.4 | 90.0*, 88.8*, 87.3 | | |
| | | 86.8, 85.8, 84.7 | | |
| | | 83.2, 80.9 | | |
| Cell. soln. from BRC-4 | 104.7 | 79.9 | 76.4, 75.0 | 61.9 |

[a] Peaks marked by * arise from the highly ordered region.

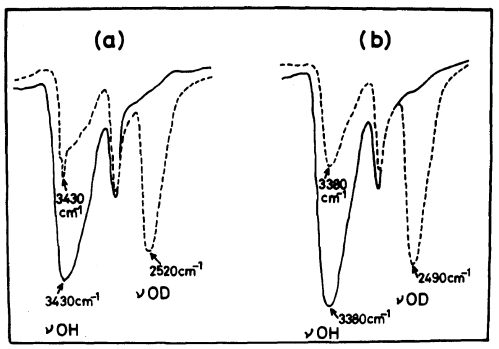


**Figure 5.** IR spectra of OH and OD stretching region for BRC-1 (a) and BRC-4 (b): solid line, before deuteration; broken line, after deuteration.

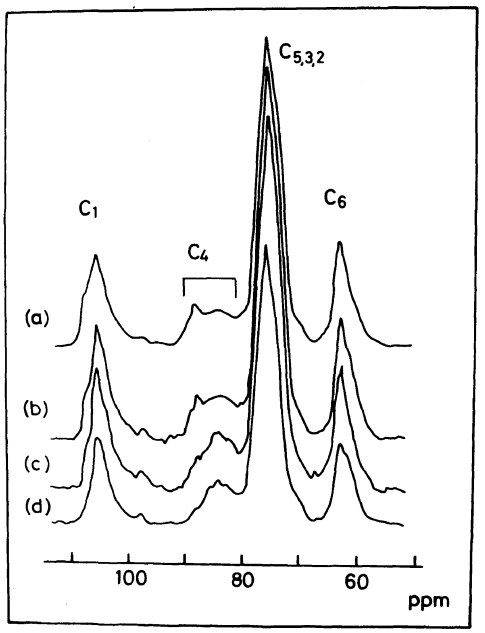


**Figure 6.** CP-MASS $^{13}$C-NMR spectra of BRC series samples: (a), BRC-1; (b), BRC-2; (c), BRC-3; (d), BRC-4.

described in experimental section.

Figure 7 shows the magnified $^{13}$C NMR spectra in the range 80—90 ppm for the $C_4$ carbon peak region, which can be approximately devided into two envelopes, as shown by the broken lines in the figure. $\chi_h$(NMR) was calculated by eq 7 and is shown in the 7th column of Table I. For the BRC-1 to BRC-4 samples, $\chi_h$(NMR) was in the range from 0.56—0.87 and that for PC-1, 0.70.

## DISCUSSION

Naturally occurring cellulose has very low solubility in aqueous alkali. Cotton dissolves by only a few or less % in a 10 wt% aqueous NaOH and pulp has about 10% solubility in such a solution at 4°C, depending on $M_v$ and $C_p$. Following the dissolution, the solutions

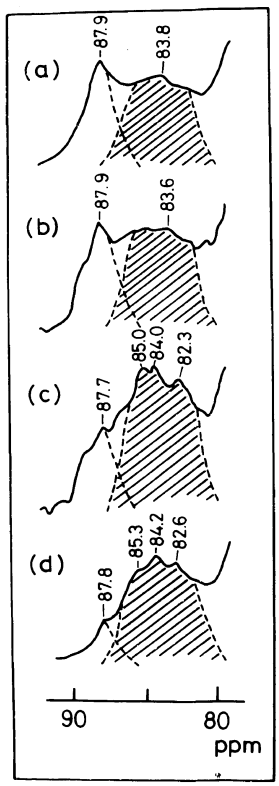


**Figure 7.** CP-MASS $^{13}C$ NMR spectra of $C_4$ carbon peak region for BRC series samples: Symbols are the same as in Figure 6. Numbers on the peaks denote peak values in ppm and the broken lines denote separation of peak areas under the peaks. Hatched line shows peak areas for higher magnetic field components.

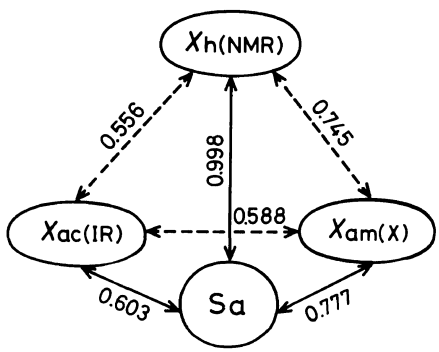


**Figure 8.** Correlations among solubility $S_a$ and the so-called amorphous content evaluated by X-ray diffraction, IR and NMR. Numbers on the lines are the correlation coefficients $\gamma$ for two arbitrarily chosen parameters.

become turbid within several minutes at 20°C. In this paper, for the first time, we were able to make celluloses, having fairly high molecular weights, to dissolve to a large extent in a dilute alkali solution at 4°C. In fact, sample BRC-5 gave a completely homogeneous solution which remained transparent and extremely stable at 20°C.

A cellulose sample, prepared physically from pulp, dissolved by as much as 58% (at $C_p=5\%$) in alkali and a significant increase in amorphous content was observed, although its $M_v$ was as low as $1.9\times10^4$ (Table I). Accordingly, an increase in the solubility of cellulose having crystal form I seems to reflect an increase in amorphous content or a decrease in $M_v$. However, according to our experience over the years, no physical treatment can produce cellulose having $S_a$ (at $C_p=5$ wt%)$>85$. Sample PC-1 was almost amorphous cellulose, as indicated by X-ray diffraction, but its $S_a$ was only 58%. Thus, $\chi_{am}(X)$ is not the only factor governing $S_a$.

Next, a correlation among $S_a$, $\chi_{am}(X)$, $\chi_{ac}(IR)$, and $\chi_h(NMR)$ were examined for samples having cellulose crystal form II so as to clarify the factors contributing to $S_a$. In this case, sample BRC-5 was excluded due to lack of $\chi_h(NMR)$ data. The results are shown in Figure 8; the numbers on the lines are the correlation coefficients $\gamma$ between two arbitrarily chosen parameters. $\gamma$ for $S_a-\chi_h(NMR)$ is really as high as 0.998 and those for $S_a-\chi_{am}(X)$ and $S_a-\chi_{ac}(IR)$ are 0.777 and 0.603, respectively. Thus, $\chi_h(NMR)$ is most closely related to $S_a$. In other words, the solubility behavior of cellulose cannot be explained by only the concepts of "crystal-amorphous" or "accessible-inaccessible." The correlation coefficients between the so-called amorphous content parameters are as follows: $\chi_{am}(X)$–$\chi_h(NMR)$; 0.745, $\chi_h(NMR)$–$\chi_{ac}(IR)$; 0.556, $\chi_{am}(X)$–$\chi_{ac}(IR)$; 0.588.

$\chi_{am}(X)$ and $\chi_h(NMR)$ shown in Table I are not well correlated and clearly inconsistent with those by Hirai *et al.*,[12] who reported

the fraction of sharp peak component in the $C_4$ carbon region (*i.e.*, $1-\chi_h$(NMR)) for natural and hydrolyzed cotton and rayon, and regenerated cellulose from a dimethylsulfoxide paraformaldehyde solution, evaluated assuming the Lorenzian type line shape, closely correlates with the degree of crystallinity determined by X-ray diffraction (*i.e.*, $1-\chi_h$(NMR)). It should be noted here that the NMR spectra do not directly reflect the supermolecular structure.

We shall now discuss the driving force responsible for splitting the $C_4$ carbon peaks into two envelopes and its physical meaning. The peak height at 87.9 ppm becomes lower for samples in the following order: BRC-1 > BRC-2 > BRC-3 > BRC-4. The peak position (87.9 ppm) for these regenerated samples is in good agreement with literature data.[7-15]

Figure 9 shows the chemical structure of a cellobiose unit. All $C_1$ and $C_4$ carbons are linked by oxygen atoms which are the center of roration accompanied by conformational change in the pyranose ring. Thus, one major factor influencing the magnetic properties of $C_1$ and $C_4$ carbons is conformational change about the $C_1'$–O–$C_4$ sequence. This change is predominantly controlled by intramolecular hydrogen bond between the neighboring glucopyranose units in a cellobiose molecule. An intramolecular hydrogen bond between the hydrogen attached to the $C_3$ carbon and ring oxygen in the neighboring glucopyranose ring causes the formation of a seven membered cyclic ether whose $C_3$ and $C_4$ carbons are located at the terminals to constitute a kind of conjugate system of $\pi$ electrons on the oxygen atoms and $\sigma$ electrons on the C–O orbitals. If the electrons in this system are mobil, $C_4$ carbon is cationized and $C_3$ carbon, anionized. If the intermolecular interaction, which can be disregarded as negligible even if it exists, is not taken into account, the electron density on the $C_4$ carbon becomes lower than that on the $C_4$ carbon not participating in the seven-membered ether on formation of the intramo-

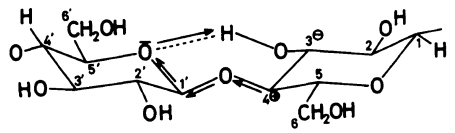

**Figure 9.** Schematic representation of the $\pi$–$\sigma$ electron conjugate system in a cellobiose unit.

lecular hydrogen bond, resulting in a shift of the $C_4$ carbon NMR peak to a lower magnetic field. Hence, we can consider a partial breakdown of the intramolecular hydrogen bonds existed in the cellulose sample to create a magnetic field about the $C_4$ carbon heterogeneously, so that its peak (and possibly as well as that of the $C_1$ carbon) produce new component in a higher magnetic field, compensating for the sharp component of the $C_4$ carbon peak. This change results in the formation of two envelopes in $C_4$ carbon peak region. The systematic change observed in Figure 7 can be reasonably interpreted by the above mechanism.

It may be concluded that a low magnetic field envelope in the $C_4$ carbon peak can be assigned to cellobiose units having fewer intramolecular hydrogen bond (*i.e.*, the region about the above-mentioned cellobiose units in cellulose molecules has a very disordered conformation). We cannot simply conclude that because there are absolutely no intramolecular hydrogen bonds, the peak narrows significantly, since a cellobiose units in cellulose molecules in the solid state can take on a large number of conformations.

On the basis of the above mechanism, variation in the lowest peak intensity among the $C_1$ carbon peaks between cellulose samples can be explained in the same manner as that in the case of the $C_4$ carbon peak, *i.e.*, the breakdown of intramolecular hydrogen bonds. The lowest peak (107.3 ppm) for the $C_1$ carbon becomes weak in the following order: BRC-1 > BRC-2 > BRC-3 > BRC-4 (Figure 6 and Table II).

Figure 10 shows the $^{13}C$ NMR spectrum for the solution of BRC-4 in NaOH–$D_2O$ (1:9,

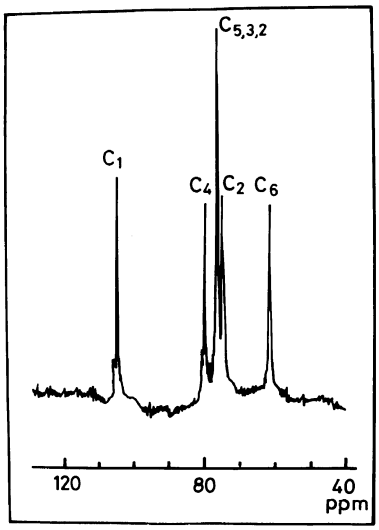


**Figure 10.** $^{13}C$ NMR spectrum for BRC-4 soltion in NaOH–$D_2O$ (1 : 9, w/w).

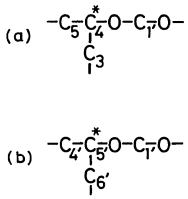


**Figure 11.** Chemical structures of two carbon–oxygen sequences about $C_4$ (a) and $C_5$ (b) following destruction of intramolecular hydrogen bonds.

w/w). Except for the $C_3$ and $C_5$ carbon peaks, all others obviously shift to a magnetic field higher than that for solid BRC-4. One $C_4$ carbon peak for the solution is located at 79.9 ppm, which is a much higher magnetic field than that (87.9 and about 84 ppm) for the original BRC-4 solid. BRC-4 dissolves molecularly in a 10 wt% aqueous NaOH without forming alcoholate and solvation with solvent[21] and hence, no intramolecular hydrogen bonds should exist in the solution. The appearance of the $C_4$ carbon peak at 79.9 ppm as a single sharp peak in the solution is quite a reasonable considering that the $C_4$ carbon peak must shift to a higher magnetic field when the intramolecular hydrogen bonds are destroyed.

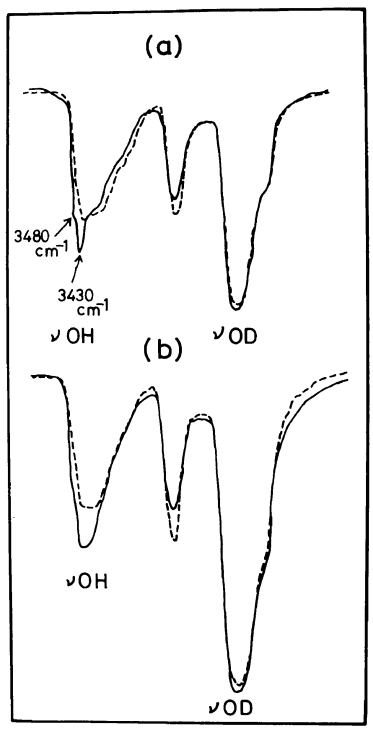


**Figure 12.** Polarized IR spectra for BRC-1 (a) and BRC-4 (b): solid line, parallel; broken line, perpendicular.

In view of the chemical structure of the two carbon–oxygen sequences about the $C_4$ and $C_5$ carbons as illustrated in Figure 11, the deshielding effect on the $C_4$ and $C_5$ carbons is estimated to be of the same order when the intramolecular hydrogen bonds are completely destroyed. Thus, the $C_4$ carbon peak should appear near the $C_5$ carbon peak. As evident from Table II, the $C_4$ carbon peak for the BRC-4 solution was observed at 79.95 ppm, and this is very close to the $C_5$ carbon peak at 76.5 ppm. Destruction of the intramolecular hydrogen bonds is also expected to cause the $C_3$ carbon peak for solid cellulose to shift to a lower magnetic field, which is the reverse of that in the case of the $C_4$ carbon peak. The main $C_3$ carbon peak for the original BRC-1 is seen at 75.1 ppm while the $C_3$ carbon peak for the BRC-4 solution in alkali is observed at 76.4 ppm. The latter is slightly lower than the former.

Additional experimental evidence supporting the formation of a higher field component of the $C_4$ carbon NMR peak by the destruction of intramolecular hydrogen bonds was obtained by IR. Figure 12 shows the polarized IR spectra of BRC-1 (a) and BRC-4 (b) (solid line; parallel, broken line; perpendicular) films after deuteration. The BRC-1 whose $S_a=52\%$ (at $C_p=5$ wt%) in a 10 wt% aqueous NaOH at 4°C shows two parallel dichroism bands at 3480 and 3430 $cm^{-1}$. These two bands are responsible for the two types of intramolecular hydrogen bonds between $O_3$–$H\cdots O_5'$ with different bond lengths (2.78 and 2.82 Å) as observed for cellulose crystal II. At a lower wave number, some perpendicular dichroism bands responsible for intermolecular hydrogen bonds appeared in sample BRC-1. In contrast, sample BRC-4 with $S_a=90\%$ does not have parallel dichroism bands at 3480 and 3430 $cm^{-1}$, but a broad parallel dichroism band at 3380 $cm^{-1}$, attributable to destruction of intramolecular hydrogen bonds. Because the IR spectra were taken after deuteration, the remaining OH stretching regions of the spectra shows the inaccessible part of the cellulose. Thus, Figure 12 shows that intramolecular hydrogen bonds are destroyed even in the inaccessible part of sample BRC-4. It may thus be concluded that almost all intramolecular hydrogen bonds are destroyed in solid sample BRC-4. Note that $\chi_h$(NMR) for BRC-4 is nearly unity (0.87). The findings also strongly suggest that the higher field component of the $C_4$ carbon peak appeared as a result of intramolecular hydrogen bond destruction.

In conclusion, it was demonstrated that cellulose whose intramolecular hydrogen bonds are completely broken or weakened dissolves in aqueous alkali and the solution thus prepared is stable over a long period of time. For a more detailed understanding of the mechanism underlying the dissolution of the cellulose reported here in alkali, additional research must be carried out.

## REFERENCES


1. For example, S. M. Neals, *J. Text. Inst.*, **20**, T373 (1920).
2. C. Beadle and H. P. Stevens, the 8th International Congress on Applied Chemistry Vol. 13, 1912, p 25.
3. H. Dillenius, *Kunstseide Zellwolle*, **22**, 314 (1940).
4. E. Schwart and W. Zimmerman, *Melliands Textilber. Int.*, **22**, 525 (1941).
5. H. Staudinger and R. Mohr, *J. Prakt. Chem.*, **158**, 233 (1941).
6. O. Eisenluth, *Cellulose Chem.*, **19**, 45 (1941).
7. R. H. Atalla, *J. Am. Chem. Soc.*, **102**, 3249 (1980).
8. W. L. Earl and D. L. Vander Hart, *J. Am. Chem. Soc.*, **102**, 3251 (1980).
9. W. L. Earl and D. L. Vander Hart, *Macromolecules*, **14**, 570 (1981).
10. F. Hirai, A. Horii, and R. Kitamaru, Preprint, 45th Chemical Society of Japan, Annual Meeting, 1982, p 1172.
11. F. Hirai, A. Horii, and R. Kitamaru, *Polym. Prepr. Jpn.*, **31**, 842 (1982).
12. F. Hirai, A. Horii, A. Akita, and R. Kitamaru, *Polym. Prepr. Jpn.*, **31**, 2519 (1982).
13. F. Hirai, A. Horii, and R. Kitamaru, Preprint, 47th Chemical Society of Japan, Annual Meeting, 1983, p 1392.
14. J. Hayashi, M. Takai, R. Tanaka, M. Hatano, and S. Nozawa, Preprint, 47th Chemical Society of Japan, Annual Meeting, 1983, p 1393.
15. G. E. Maciel, *Macromolecules*, **15**, 686 (1982).
16. W. Brown and R. Wikström, *Eur. Polym. J.*, **1**, 1 (1966).
17. L. Segal, *Text. Res. J.*, **29**, 786 (1959).
18. J. Mann and H. J. Marrinan, *Trans. Faraday Soc.*, **52**, 492 (1956).
19. J. Hayashi, Preprint, Cellulose Micro Symposium, Sapporo, 1983, p 21.
20. For example, J. Blackwell and R. H. Marchessault, "Cellulose and Cellulose Derivatives," Part IV, Bikales and Segal Ed., John Wiley & Sons Inc., New York, N. Y., 1971, Chapter XIII, p 18.
21. K. Kamide, K. Okajima, T. Matsui, and T. Abe, unpublished results.